

Communication-efficient Vertical Federated Learning via Compressed Error Feedback

Pedro Valdeira*[†]
CMU & IST

João Xavier[†]
IST

Cláudia Soares[‡]
NOVA

Yuejie Chi*
CMU

June 21, 2024

Abstract

Communication overhead is a known bottleneck in federated learning (FL). To address this, lossy compression is commonly used on the information communicated between the server and clients during training. In horizontal FL, where each client holds a subset of the samples, such communication-compressed training methods have recently seen significant progress. However, in their vertical FL counterparts, where each client holds a subset of the features, our understanding remains limited. To address this, we propose an error feedback compressed vertical federated learning (EFVFL) method to train split neural networks. In contrast with previous communication-compressed methods for vertical FL, EFVFL does not require a vanishing compression error for the gradient norm to converge to zero for smooth nonconvex problems. By leveraging error feedback, our method can achieve a $\mathcal{O}(1/T)$ convergence rate in the full-batch case, improving over the state-of-the-art $\mathcal{O}(1/\sqrt{T})$ rate under $\mathcal{O}(1/\sqrt{T})$ compression error, and matching the rate of uncompressed methods. Further, when the objective function satisfies the Polyak-Łojasiewicz inequality, our method converges linearly. In addition to improving convergence rates, our method also supports the use of private labels. Numerical experiments show that EFVFL significantly improves over the prior art, confirming our theoretical results.

1 Introduction

Federated learning (FL) is a machine learning paradigm where a set of clients holding local datasets collaborate to train a model without exposing their local data (McMahan et al., 2017). FL can be divided into two categories, based on how the data is partitioned across the clients: *horizontal* FL, where each client holds a different set of samples but all clients share the same features, and *vertical* FL, where each client holds a different subset of features but all clients share the same samples. Note that we cannot gather and redistribute the data because it must remain at the clients. Thus, we do not choose under which category a given task falls. Rather, the category is a consequence of how the data arises.

In this work, we focus on vertical FL (VFL) (Liu et al., 2024). In VFL, a global dataset $\mathcal{D} = \{\xi_n\}_{n=1}^N$ with N samples is partitioned by features across a set of clients $[K] := \{1, \dots, K\}$. Each sample has K disjoint blocks of features $\xi_n = (\xi_{n1}, \dots, \xi_{nK})$ and the local dataset of each client $k \in [K]$ is $\mathcal{D}_k = \{\xi_{nk}\}_{n=1}^N$, where $\mathcal{D} = \bigcup_k \mathcal{D}_k$. Since different datasets \mathcal{D}_k have different features, VFL suits collaborations of clients with complementary types of information, who tend to have fewer competing interests. This can lead to a greater incentive to collaborate, compared to horizontal FL. A common application of VFL is in settings where multiple entities own distinct features concerning a shared set of users and seek to collaboratively train a predictor; for example, WeBank partners with other companies to jointly build a risk model from data regarding shared customers (Cheng et al., 2020).

To jointly train a model from $\{\mathcal{D}_k\}$ without sharing local data, split neural networks (Ceballos et al., 2020) are often considered. To learn the parameters \mathbf{x} of such models, we aim to solve the following nonconvex

*Department of Electrical and Computer Engineering, Carnegie Mellon University; email: pvaldeira@cmu.edu.

[†]Institute for Systems and Robotics, Instituto Superior Técnico.

[‡]Department of Computer Science, NOVA School of Science and Technology.

⁴A preliminary version of this work was accepted for publication at EUSIPCO 2024 (Valdeira et al., 2024).

optimization problem:

$$\min_{\mathbf{x} \in \mathbb{R}^d} f(\mathbf{x}) := \frac{1}{N} \sum_{n=1}^N \phi_n(\mathbf{x}_0, \mathbf{h}_{1n}(\mathbf{x}_1), \dots, \mathbf{h}_{Kn}(\mathbf{x}_K)), \quad (1)$$

where $\mathbf{x} := (\mathbf{x}_0, \mathbf{x}_1, \dots, \mathbf{x}_K)$. Here, $\mathbf{h}_{kn}(\mathbf{x}_k) := \mathbf{h}_k(\mathbf{x}_k; \boldsymbol{\xi}_{nk})$ is the local model of client $k \in [K]$, which is parameterized by \mathbf{x}_k and extracts an (often lower-dimensional) representation of $\boldsymbol{\xi}_{nk}$. These representations, or embeddings, are then sent to the server. The server, in turn, uses $\{\mathbf{h}_{kn}(\mathbf{x}_k)\}_{k=1}^K$ as input to ϕ_n , which corresponds to the composition of the loss function and the server model and is parameterized by \mathbf{x}_0 .¹

Most FL methods, including ours, assume that the server can communicate with all the clients and that the clients do not communicate with each other. These methods typically require many rounds of client-server communications. Such communications can significantly slow down training. In fact, they can become the main bottleneck during training (Dean et al., 2012; Lian et al., 2017). To address this, a plethora of communication-efficient FL methods have been proposed. In particular, a popular technique to mitigate the communication overhead is lossy compression. Compression operators, or simply compressors, are operators that map a given vector into another vector that is easier to communicate (that is, requires fewer bits).

Optimization methods employing communication compression have seen great success (Seide et al., 2014; Alistarh et al., 2017). Most of these works focus on the prevalent horizontal FL setup and thus consider *gradient* compression, as these are the vectors being communicated in the horizontal setting (Alistarh et al., 2018; Stich et al., 2018). Yet, in vertical FL, the clients send *representations* $\{\mathbf{h}_{kn}(\mathbf{x}_k)\}$ instead. In contrast to gradient compression, compressing these intermediate representations leads the compression-induced error to undergo a nonlinear function ϕ_n before impacting gradient-based updates. Thus, compression in VFL is not covered by these works and our understanding of it remains limited. In fact, to the best of our knowledge, Castiglia et al. (2022) is the only work providing convergence guarantees for compressed VFL. Yet, Castiglia et al. (2022) employs a direct compression method, requiring the compression error to go to zero as the number of gradient steps T increases, achieving a $\mathcal{O}(1/\sqrt{T})$ rate when the compression error is $\mathcal{O}(1/\sqrt{T})$. This makes the method in Castiglia et al. (2022) unsuitable for applications with strict per-round communication limitations, such as bandwidth constraints, and leads to the following question:

Can we design a communication-compressed VFL method that preserves the convergence rate of uncompressed methods without decreasing the amount of compression as training progresses?

1.1 Our contributions

In this work, we answer the question above in the affirmative. Our main contributions are as follows.

- We propose error feedback compressed VFL (EFVFL), which leverages an error feedback technique to improve the stability of communication-compressed training in VFL.
- We show that our method achieves a convergence rate of $\mathcal{O}(1/T)$ for nonconvex objectives under nonvanishing compression error, improving over the state-of-the-art $\mathcal{O}(1/\sqrt{T})$ rate under $\mathcal{O}(1/\sqrt{T})$ compression error of Castiglia et al. (2022), and matching the rate of the centralized setting. We further show that, under the Polyak-Łojasiewicz (PL) inequality, our method converges linearly, thus obtaining the first linearly convergent compressed VFL method. Unlike the method in Castiglia et al. (2022), EFVFL supports the use of private labels, broadening its applicability.
- We run numerical experiments and observe empirically that our method improves the state-of-the-art, achieving a better communication efficiency than existing methods.

1.2 Related work

Communication-efficient FL. The aforementioned communication bottleneck in FL (Lian et al., 2017) makes communication-efficient methods a particularly active area of research. FL methods often employ multiple local updates between rounds of communication, use only a subset of the clients at a time (McMahan

¹The server often aggregates the representations \mathbf{h}_{kn} via some nonparameterized operation (for example, a sum or an average) before inputting them into the server model. We consider this aggregation to be included in ϕ_n .

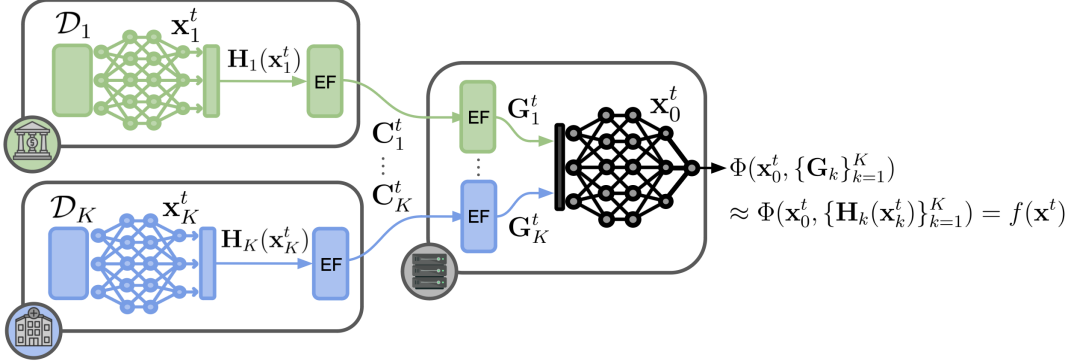


Figure 1: A split neural network with K clients using error feedback (EF) compression for a forward pass. The clients can include, for example, a bank and a hospital, as illustrated.

et al., 2017), or even update the global model asynchronously (Xie et al., 2019). Another line of research considers fully decentralized methods (Lian et al., 2017), dispensing with the server and, instead, exploiting communications between clients. This can alleviate the bandwidth limit ensuing from the centralized role of the server. Another popular technique is lossy compression, which is the focus of this work.

Communication-compressed optimization methods can exploit different families of compressors. A popular choice is the family of *unbiased* compressors (Alistarh et al., 2017), which is appealing in that its properties facilitate the theoretical analysis of the resulting methods. Yet, some widely adopted compressors do not belong to this class, such as top- k sparsification (Alistarh et al., 2018; Stich et al., 2018) and deterministic rounding (Sapio et al., 2021). Thus, the broader family of *contractive* compressors (Beznosikov et al., 2023) has recently attracted a lot of attention. Yet, methods employing them for direct compression are often prone to instability or even divergence (Beznosikov et al., 2023). To address this, error feedback techniques have been proposed; first, as a heuristic (Seide et al., 2014), but, more recently, significant progress has been made on our theoretical understanding of the application of these methods to gradient compression (Stich et al., 2018; Alistarh et al., 2018; Richtárik et al., 2021). In the horizontal setting, some works have combined error feedback compression with the aforementioned communication-efficient techniques, such as communication-compressed fully decentralized methods (Koloskova et al., 2019; Zhao et al., 2022).

Vertical FL. To mitigate the communication bottleneck in VFL, we often employ techniques akin to those used in horizontal FL. In particular, Liu et al. (2022) performed multiple local updates between communication rounds, Chen et al. (2020) updated the local models asynchronously, and Ying et al. (2018) proposed a fully decentralized approach. Recently, Valdeira et al. (2023) proposed a semi-decentralized method leveraging both client-server and client-client communications to avoid the slow convergence of fully-decentralized methods on large and sparse networks while alleviating the server bottleneck.

In this work, we focus on communication-compressed methods tailored to VFL. While, as mentioned above, most work in communication-compressed methods focuses on gradient compression and thus does not apply directly to VFL, recently, a few empirical works on VFL have employed compression. Namely, Khan et al. (2022) compressed the local data before sending it to the server, where the model is trained, and Li et al. (2020) proposed an asynchronous method with bidirectional (sparse) gradient compression. Nevertheless, Castiglia et al. (2022), where direct compression is used, is the only work on compressed VFL with theoretical guarantees. For a more detailed discussion on VFL, see Liu et al. (2024); Yang et al. (2023).

2 Preliminaries

We now define the class of contractive compressors, which we consider throughout this paper.

Definition 1 (Contractive compressor). *A map $\mathcal{C}: \mathbb{R}^d \mapsto \mathbb{R}^d$ is a contractive compressor if there exists*

$\alpha \in (0, 1]$ such that,²

$$\forall \mathbf{v} \in \mathbb{R}^d: \quad \mathbb{E} \|\mathcal{C}(\mathbf{v}) - \mathbf{v}\|^2 \leq (1 - \alpha) \|\mathbf{v}\|^2, \quad (2)$$

where the expectation is taken with respect to the (possible) randomness in \mathcal{C} .

2.1 Error feedback

Error feedback is useful when using compressed communications to send a sequence of vectors $\{\mathbf{v}^t\}$ which we expect to converge. Unlike direct compression, where each \mathbf{v}^t is compressed independently and $\mathcal{C}(\mathbf{v}^t)$ acts as a surrogate for \mathbf{v}^t , in error feedback compression, an estimate \mathbf{s}^t is used as a surrogate. This surrogate is initialized as $\mathbf{s}^0 = \mathcal{C}(\mathbf{v}^0)$ and is updated recursively as follows:

$$\forall t \geq 0: \quad \mathbf{s}^{t+1} = \mathbf{s}^t + \mathcal{C}(\mathbf{v}^{t+1} - \mathbf{s}^t). \quad (3)$$

Unlike $\mathcal{C}(\mathbf{v}^t)$, \mathbf{s}^t is not necessarily in the range of \mathcal{C} . For example, if \mathcal{C} uses sparsification, $\mathcal{C}(\mathbf{v}^t)$ must be sparse, but \mathbf{s}^t may not. Accumulating the compressed error of our surrogate allows \mathbf{s}^t to “track” \mathbf{v}^t . Also, since the updates $\mathcal{C}(\mathbf{v}^{t+1} - \mathbf{s}^t)$ are compressed, we preserve the communication cost of direct compression. Surrogate \mathbf{s}^t is updated at both the machine (that is, client or server) sending the information and the one receiving it. Note that \mathbf{s}^t can be seen as a Markovian compressor, as it depends only on \mathbf{v}^t and \mathbf{s}^{t-1} .

2.2 Problem setup

Let $\mathbf{h}_{0n}(\mathbf{x}_0) = \mathbf{x}_0$ and $\mathbf{h}_n(\mathbf{x}) = (\mathbf{h}_{0n}(\mathbf{x}_0), \dots, \mathbf{h}_{Kn}(\mathbf{x}_K)) \in \mathbb{R}^E$ where $\mathbf{h}_{kn}(\mathbf{x}_k) \in \mathbb{R}^{E_k}$ and $E = \sum_{k=0}^K E_k$, for all n . Further, let

$$\mathbf{H}_k(\mathbf{x}_k) = \begin{bmatrix} \mathbf{h}_{k1}(\mathbf{x}_k) \\ \vdots \\ \mathbf{h}_{kN}(\mathbf{x}_k) \end{bmatrix} \in \mathbb{R}^{N \times E_k}$$

and

$$\mathbf{H}(\mathbf{x}) := [\mathbf{H}_0(\mathbf{x}_0), \mathbf{H}_1(\mathbf{x}_1), \dots, \mathbf{H}_K(\mathbf{x}_K)] \in \mathbb{R}^{N \times E}.$$

Further, we define $\Phi: \mathbb{R}^{N \times E} \mapsto \mathbb{R}$ as follows:

$$f(\mathbf{x}) = \frac{1}{N} \sum_{n=1}^N \phi_n(\mathbf{h}_n(\mathbf{x})) =: \Phi(\mathbf{H}(\mathbf{x})).$$

Throughout most of the paper, we assume that ϕ_n contains the label of ξ_n and that ϕ_n is known by all the clients and the server. This assumption, known as “relaxed protocol” (Liu et al., 2024), is sometimes made in VFL (Hu et al., 2019; Castiglia et al., 2022, 2023) and has applications, for example, in credit score prediction. We also address the case of private labels, proposing a modified version of our method for that setting in Section 3.1.

We assume that f has an optimal value $f^* := \min_{\mathbf{x}} f(\mathbf{x}) > -\infty$ and make the following assumptions, where ∇ denotes not only the gradient of scalar-valued functions but, more generally, the derivative of a (possibly multidimensional) map.

Assumption 1 (Smoothness). *A function $h: \mathbb{R}^d \mapsto \mathbb{R}$ is L -smooth if there exists a positive constant L such that*

$$\forall \mathbf{x}, \mathbf{y} \in \mathbb{R}^d: \quad \|\nabla h(\mathbf{x}) - \nabla h(\mathbf{y})\| \leq L \|\mathbf{x} - \mathbf{y}\|. \quad (A1)$$

We assume f is L_f -smooth and Φ is L_Φ -smooth and let $L = \max\{L_f, L_\Phi\}$.

Assumption 2 (Bounded derivative). *Map $\mathbf{F}: \mathbb{R}^{p_1} \mapsto \mathbb{R}^{p_2 \times p_3}$ has a bounded derivative if there exists a positive constant H such that*

$$\forall \mathbf{x} \in \mathbb{R}^{p_1}: \quad \|\nabla \mathbf{F}(\mathbf{x})\| \leq H, \quad (A2)$$

where $\|\nabla \mathbf{F}(\mathbf{x})\|$ is the Euclidean norm of the third-order tensor $\nabla \mathbf{F}(\mathbf{x})$. We assume (A2) holds for $\{\mathbf{H}_k\}_{k=0}^K$.

²In Definition 1, we use a common, simplified notation, omitting the randomness in $\mathcal{C}: \mathbb{R}^d \times \Omega \rightarrow \mathbb{R}^d$. We assume that the randomness ω in $\mathcal{C}(\mathbf{v}, \omega)$ at different applications of \mathcal{C} is independent.

Note that, in Assumption 2, we do *not* assume that our objective function f has a bounded gradient. We only require the local representation-extracting maps $\{\mathbf{H}_k\}$ to have a bounded derivative. The same assumption is also made in Castiglia et al. (2022).

3 Proposed method

To solve Problem (1) with a gradient-based method, we need to perform a forward and a backward pass at each step t to compute the gradient of our objective function. In VFL, a standard uncompressed algorithm employing a single local update per communication round is mathematically equivalent to gradient descent.³ This algorithm, which our method recovers if we set \mathcal{C} to be the identity map, is as follows:

- In the forward pass, each client k computes $\mathbf{H}_k(\mathbf{x}^t)$ and sends it to the server, which then computes $f(\mathbf{x}^t) = \Phi(\mathbf{H}(\mathbf{x}^t))$.
- In the backward pass, first, the server backpropagates through Φ , obtaining $\nabla_0\Phi(\mathbf{x}_0^t, \{\mathbf{H}_k(\mathbf{x}_k^t)\}_{k=1}^K) = \nabla_0 f(\mathbf{x}^t)$ and $\nabla_k\Phi(\{\mathbf{H}_k(\mathbf{x}_k^t)\})$, for all k , where ∇_k denotes the derivative with respect to block k . The former is used to update \mathbf{x}_0^t , while the latter is sent to each client k , which uses this derivative to continue backpropagation over its local model, allowing it to compute $\nabla_k f(\mathbf{x}^t)$.

We repeat these steps until convergence. Let us now cover the general case, where \mathcal{C} may not be the identity map.

Forward pass. An exact forward pass would require each client k to send $\mathbf{H}_k(\mathbf{x}_k^t)$ to the server, bringing a significant communication overhead. To address this, in our method, the server model does not have as input $\mathbf{H}_k(\mathbf{x}_k^t)$, but rather a surrogate for it, \mathbf{G}_k^t , which is initialized as $\mathbf{G}_k^0 = \mathcal{C}(\mathbf{H}_k(\mathbf{x}_k^0))$ and is updated as follows, as in (3):

$$\forall k \in [K]: \quad \mathbf{G}_k^t := \mathbf{G}_k^{t-1} + \mathbf{C}_k^t \quad \text{where} \quad \mathbf{C}_k^t := \mathcal{C}(\mathbf{H}_k(\mathbf{x}_k^t) - \mathbf{G}_k^{t-1}).$$

This requires keeping \mathbf{G}_k^t , of size $N \times E_k$, in memory at client k and at the server. (Note that \mathbf{G}_k^t is often smaller than the local dataset \mathcal{D}_k .) The server thus computes the function $\Phi(\mathbf{x}_0^t, \mathbf{G}_1^t, \dots, \mathbf{G}_K^t)$, which acts as a surrogate for the original objective $f(\mathbf{x}^t) = \Phi(\mathbf{x}_0^t, \mathbf{H}_1(\mathbf{x}_1^t), \dots, \mathbf{H}_K(\mathbf{x}_K^t))$, as illustrated in Figure 1.

Backward pass. The server performs a backward pass over the server model, obtaining $\nabla_0\Phi(\mathbf{x}_0^t, \{\mathbf{G}_k^t\}_{k=1}^K)$, which it uses as a surrogate for $\nabla_0\Phi(\mathbf{x}_0^t, \{\mathbf{H}_k(\mathbf{x}_k^t)\}_{k=1}^K) = \nabla_0 f(\mathbf{x}^t)$ to update \mathbf{x}_0^t . Similarly, to update each local model \mathbf{x}_k^t , for $k \in [K]$, we want client k to have a surrogate for

$$\nabla_k f(\mathbf{x}^t) = \sum_{i,j=1}^{N, E_k} [\nabla_k\Phi(\{\mathbf{H}_k(\mathbf{x}_k^t)\}_{k=0}^K)]_{ij} [\nabla\mathbf{H}_k(\mathbf{x}_k^t)]_{ij}.$$

However, while $\nabla\mathbf{H}_k(\mathbf{x}_k^t)$ can be computed at each client k , the $\nabla_k\Phi$ term cannot, as client k does not have access to $\mathbf{H}_\ell(\mathbf{x}_\ell^t)$, for $\ell \neq k$. So, we instead use the following surrogate for $\nabla_k f(\mathbf{x}^t)$:

$$\mathbf{g}_k^t := \sum_{i,j=1}^{N, E_k} [\tilde{\nabla}_k^t\Phi]_{ij} [\nabla\mathbf{H}_k(\mathbf{x}_k^t)]_{ij}, \quad (4)$$

where $\tilde{\nabla}_k^t\Phi := \nabla_k\Phi(\dots, \mathbf{G}_{k-1}^t, \mathbf{H}_k(\mathbf{x}_k^t), \mathbf{G}_{k+1}^t, \dots)$. Since the server does not hold $\mathbf{H}_k(\mathbf{x}_k^t)$, it cannot compute $\tilde{\nabla}_k^t\Phi$. Thus, the server broadcasts $\{\mathbf{C}_k^t\}_{k=0}^K$, so that each client k , which does hold $\mathbf{H}_k(\mathbf{x}_k^t)$, can compute $\{\mathbf{G}_\ell^t\}_{\ell \neq k}$ and use it to perform a forward and a backward pass over the server model locally, obtaining $\tilde{\nabla}_k^t\Phi$. Thus, while the forward pass only requires the error feedback module at each client k to hold the estimate \mathbf{G}_k^t , when we account for the backward pass too, each machine $k \in \{0, 1, \dots, K\}$ must hold $\{\mathbf{G}_\ell^t\}_{\ell=0}^K$. We write our update as:

$$\mathbf{x}^{t+1} = \mathbf{x}^t - \eta \mathbf{g}^t \quad \text{where} \quad \mathbf{g}^t := (\mathbf{g}_0^t, \dots, \mathbf{g}_K^t)$$

and η is the stepsize.

³When performing multiple local updates, we lose this mathematical equivalence. In that case, we instead get a parallel (block) coordinate descent method where the simultaneous updates use stale information about the other blocks of variables.

Algorithm 1: EFVFL

- Input:** initial point \mathbf{x}^0 , stepsize η , and initial surrogates $\{\mathbf{G}_k^0 = \mathcal{C}(\mathbf{H}_k(\mathbf{x}_k^0))\}$.
- 1 **for** $t = 0, \dots, T - 1$ **do**
 - 2 Update $\mathbf{x}_k^{t+1} = \mathbf{x}_k^t - \eta \tilde{\mathbf{g}}_k^t$ in parallel, for $k \in \{0, 1, \dots, K\}$, based on a shared sample $\mathcal{B}^t \subseteq [N]$.
 - 3 Compute and send $\mathbf{C}_k^{t+1} = \mathcal{C}(\mathbf{H}_k(\mathbf{x}_k^{t+1}) - \mathbf{G}_k^t)$ to the server in parallel, for $k \in [K]$.
 - 4 Server broadcasts $\{\mathbf{C}_k^{t+1}\}_{k=0}^K$ to all clients.
 - 5 Update $\mathbf{G}_k^{t+1} = \mathbf{G}_k^t + \mathbf{C}_k^{t+1}$ in parallel, for $k \in \{0, 1, \dots, K\}$.
-

Mini-batch. For the sake of computation efficiency, we further allow for the use of mini-batch approximations of the objective. Without compression, or with direct compression, the use of mini-batches allows client k to send only the entries of $\mathbf{H}_k(\mathbf{x}_k)$ corresponding to mini-batch $\mathcal{B} \subseteq [N]$, of size B , denoted by $\mathbf{H}_{k\mathcal{B}}(\mathbf{x}_k) \in \mathbb{R}^{B \times E_k}$, instead of $\mathbf{H}_k(\mathbf{x}_k) \in \mathbb{R}^{N \times E_k}$. Yet, our method provides all machines with an estimate for all the entries of $\{\mathbf{H}_k(\mathbf{x}_k)\}$ at all times, the error feedback states $\{\mathbf{G}_k\}$. Therefore, our communications, needed to update \mathbf{G}_k , may not depend on N and B at all. This is determined by our choice of \mathcal{C} .

Our mini-batch surrogates depend on the entries of $\mathbf{H}_k(\mathbf{x}_k)$ and \mathbf{G}_k corresponding to \mathcal{B} , $\mathbf{H}_{k\mathcal{B}}(\mathbf{x}_k)$, and $\mathbf{G}_{k\mathcal{B}}$. (Note that $\mathbf{H}_{0\mathcal{B}}(\mathbf{x}_0) = \mathbf{H}_0(\mathbf{x}_0)$ and $\mathbf{G}_{0\mathcal{B}}^t = \mathbf{G}_0^t$.) Thus, we approximate the partial derivative of the mini-batch function $f_{\mathcal{B}}(\mathbf{x}) = \Phi_{\mathcal{B}}(\{\mathbf{H}_{k\mathcal{B}}(\mathbf{x}_k)\}) = \frac{1}{B} \sum_{n \in \mathcal{B}} \phi_n(\mathbf{h}_n(\mathbf{x}))$ with respect to \mathbf{x}_k by:

$$\tilde{\mathbf{g}}_k^t := \sum_{i \in \mathcal{B}^t} \sum_{j=1}^{E_k} \left[\tilde{\nabla}_k^t \Phi_{\mathcal{B}^t} \right]_{ij} [\nabla \mathbf{H}_{k\mathcal{B}^t}(\mathbf{x}_k^t)]_{ij},$$

where $\tilde{\nabla}_k^t \Phi_{\mathcal{B}^t} := \nabla_k \Phi_{\mathcal{B}^t}(\dots, \mathbf{G}_{k-1, \mathcal{B}^t}^t, \mathbf{H}_{k\mathcal{B}^t}(\mathbf{x}_k^t), \mathbf{G}_{k+1, \mathcal{B}^t}^t, \dots)$. We write the mini-batch version of the update as:

$$\mathbf{x}^{t+1} = \mathbf{x}^t - \eta \tilde{\mathbf{g}}^t \quad \text{where} \quad \tilde{\mathbf{g}}^t := (\tilde{\mathbf{g}}_0^t, \dots, \tilde{\mathbf{g}}_K^t).$$

We now describe our method, which we summarize in Algorithm 1.

- **Initialization:** We initialize our model parameters as \mathbf{x}^0 . Each machine $k \in \{0, 1, \dots, K\}$ must hold \mathbf{x}_k^0 and our compression estimates $\{\mathbf{G}_k^0 = \mathcal{C}(\mathbf{H}_k(\mathbf{x}_k^0))\}_{k=0}^K$.
- **Model parameters update:** In parallel, all machines $k \in \{0, 1, \dots, K\}$ take a (stochastic) coordinate descent step with respect to their local surrogate objective, updating $\mathbf{x}_k^{t+1} = \mathbf{x}_k^t - \eta \tilde{\mathbf{g}}_k^t$ based on a shared batch \mathcal{B}^t , sampled locally at each client following a shared seed.
- **Compressed communications:** All clients $k \in [K]$ compute \mathbf{C}_k^{t+1} and send it to the server, who broadcasts $\{\mathbf{C}_k^{t+1}\}$.
- **Compression estimates update:** Lastly, all machines $k \in \{0, 1, \dots, K\}$ use the compressed error feedback $\{\mathbf{C}_k^{t+1}\}$ to update their (matching) compression estimates $\{\mathbf{G}_k^t\}$.

Note that, in the absence of compression (that is, if \mathcal{C} is the identity operator), each client k must send \mathbf{C}_k^{t+1} , of size $N \times E_k$, at each iteration. Further, the server must broadcast $\{\mathbf{C}_k^{t+1}\}_{k=0}^K$. Thus, the total communication complexity of EFVFL in the absence of compression is $\mathcal{O}(N \cdot E \cdot T)$. When compression is used, $N \cdot E$ is replaced by some smaller amount which depends on the compression mechanism. For example, for top- k sparsification (defined in Section 5), the communication complexity is reduced to $\mathcal{O}(k \cdot T)$.

In Algorithm 1, we formulate our method in a general setting which allows for the compression of both $\{\mathbf{H}_k(\mathbf{x}_k)\}_{k=1}^K$ and \mathbf{x}_0 . This setting is covered by our analysis in Section 4. However, in general, the bottleneck lies in the uplink (client-to-server) communications, rather than the server broadcasting (Haddadpour et al., 2021). Therefore, our experiments in Section 5 focus on the compression of $\{\mathbf{H}_k(\mathbf{x}_k)\}_{k=1}^K$, rather than \mathbf{x}_0 .

3.1 Adapting our method for handling private labels

In this section, we propose an adaptation of EFVFL to allow for private labels. That is, we remove the assumption that all clients hold ϕ_n , which contains the label of ξ_n . Instead, only the server holds the labels. Further, in this adaptation, the parameters of the server model, \mathbf{x}_0 , are not shared with the clients either.

Algorithm 2: EFVFL with private labels

- Input :** initial point \mathbf{x}^0 , stepsize η , and initial surrogates $\{\mathbf{G}_k^0 = \mathcal{C}(\mathbf{H}_k(\mathbf{x}_k^0))\}$.
- 1 **for** $t = 0, \dots, T - 1$ **do**
 - 2 Update $\mathbf{x}_k^{t+1} = \mathbf{x}_k^t - \eta \tilde{\nabla}_k^t$ in parallel, for $k \in \{0, 1, \dots, K\}$, based on a shared sample $\mathcal{B}^t \subseteq [N]$.
 - 3 Compute and send $\mathbf{C}_k^{t+1} = \mathcal{C}(\mathbf{H}_k(\mathbf{x}_k^{t+1}) - \mathbf{G}_k^t)$ to the server in parallel, for $k \in [K]$.
 - 4 Server sends $\nabla_k \Phi_{\mathcal{B}^t}(\mathbf{H}_{0\mathcal{B}^t}(\mathbf{x}_0^t), \{\mathbf{G}_{j\mathcal{B}^t}^t\}_{j=1}^K)$ to client k , in parallel, for $k \in \{0, 1, \dots, K\}$.
 - 5 Update $\mathbf{G}_k^{t+1} = \mathbf{G}_k^t + \mathbf{C}_k^{t+1}$ in parallel, for $k \in \{0, 1, \dots, K\}$.
-

Note that, without holding ϕ_n , the clients cannot perform the entire forward pass locally. Instead, in this setting, the forward and backward pass over ϕ_n take place at the server, while the forward and backward pass over $\mathbf{H}_k(\mathbf{x}_k)$ takes place at client k . More precisely, in the forward pass, each client k sends \mathbf{C}_k to the server, who holds \mathbf{x}_0 and the labels, and can thus compute the loss. Then, for the backward pass, the server backpropagates over its model and sends only the derivative of the loss function with respect to \mathbf{G}_k to each client k . This requires replacing our surrogate of $\nabla_k f(\mathbf{x}^t)$ in (4), which uses the exact local representation $\mathbf{H}_k(\mathbf{x}_k)$ at each client, by one based on our error feedback surrogates:

$$\nabla_k^t := \sum_{i,j=1}^{N, E_k} [\nabla_k \Phi(\mathbf{H}_0(\mathbf{x}_0^t), \{\mathbf{G}_j^t\}_{j=1}^K)]_{ij} [\nabla \mathbf{H}_k(\mathbf{x}_k^t)]_{ij}. \quad (5)$$

Note that we do not backpropagate through the error-feedback update.

More generally, we use the following (possibly) mini-batch update vector:

$$\tilde{\nabla}_k^t := \sum_{i \in \mathcal{B}^t} \sum_{j=1}^{E_k} [\nabla_k \Phi_{\mathcal{B}^t}(\mathbf{H}_{0\mathcal{B}^t}(\mathbf{x}_0^t), \{\mathbf{G}_{j\mathcal{B}^t}^t\}_{j=1}^K)]_{ij} [\nabla \mathbf{H}_{k\mathcal{B}^t}(\mathbf{x}_k^t)]_{ij}.$$

We summarize the adaption of the EFVFL method to the private labels setting in Algorithm 2.

Allowing for private labels broadens the range of applications for our method, since many VFL applications require not only private features, but also private labels, rendering any method requiring public labels inapplicable. However, as we will see in Section 5.2, using surrogate (5) instead of (4) can slow down convergence. Further, unlike Algorithm 1, which can be easily extendable to allow for multiple local updates at the clients between rounds of communication, Algorithm 2 works only for a single local update. This is because, for an VFL algorithm to perform multiple local updates, ϕ_n and \mathbf{x}_0 must be available at the clients, so that the forward and backward passes over the server model and the loss function can be performed locally after each update.

4 Convergence guarantees

In this section, we provide convergence guarantees for EFVFL. We present our results for Algorithm 1 only, rather than stating them again for Algorithm 2, since they exhibit only a minor difference in Lemma 1 and in main theorem, where the constant K is replaced with $K + 1$. We defer the details to Appendix A.

First, let us define the following sigma-algebra

$$\mathcal{F}_t := \sigma(\mathbf{G}^0, \mathbf{x}^1, \mathbf{G}^1, \dots, \mathbf{x}^t, \mathbf{G}^t),$$

where $\mathbf{G}^t := \{\mathbf{G}_0^t, \dots, \mathbf{G}_K^t\}$. For the sake of conciseness, we further let $\mathbb{E}_{\mathcal{F}}$ denote the conditional expectation $\mathbb{E}[\cdot | \mathcal{F}]$ with sigma-algebra \mathcal{F} . We use the following assumptions on our stochastic update vector $\tilde{\mathbf{g}}^t$ and the use of mini-batches.

Assumption 3 (Unbiased). *We assume that our stochastic update vector is unbiased:*

$$\forall(\mathbf{x}, t) \in \mathbb{R}^d \times \{0, 1, \dots, T - 1\}: \quad \mathbb{E}_{\mathcal{F}_t}[\tilde{\mathbf{g}}^t] = \mathbf{g}^t. \quad (\text{A3})$$

Assumption 4 (Bounded variance). We assume that there exists a constant $\sigma \geq 0$ such that

$$\forall(\mathbf{x}, t) \in \mathbb{R}^d \times \{0, 1, \dots, T-1\}: \quad \mathbb{E}_{\mathcal{F}_t} \|\tilde{\mathbf{g}}^t - \mathbf{g}^t\|^2 \leq \frac{\sigma^2}{B}. \quad (\text{A4})$$

We now present Lemma 1 and Lemma 2, which we will use to prove our main theorems. We let $D^t := \sum_{k=0}^K \|\mathbf{G}_k^t - \mathbf{H}_k(\mathbf{x}_k^t)\|^2$ denote the total distortion (caused by compression) at time t .

Lemma 1 (Surrogate offset bound). If Φ is L -smooth (A1) and $\{\mathbf{H}_k\}$ have bounded derivatives (A2), then, for all $t \geq 0$,

$$\|\mathbf{g}^t - \nabla f(\mathbf{x}^t)\|^2 \leq KH^2L^2D^t. \quad (6)$$

Proof. See Appendix B.1. □

Lemma 2 (Recursive distortion bound). Let $\{\mathbf{x}^t\}$ be a sequence generated by Algorithm 1. If \mathcal{C} is a contractive compressor (2), $\{\mathbf{H}_k\}$ have bounded derivatives (A2), and (A3) and (A4) hold, then, for all $t \geq 0$ and $\epsilon > 0$:

$$\mathbb{E}D^{t+1} \leq (1-\alpha)(1+\epsilon)\mathbb{E}D^t + (1-\alpha)(1+\epsilon^{-1})\eta^2H^2 \left(\mathbb{E}\|\mathbf{g}^t\|^2 + \frac{\sigma^2}{B} \right). \quad (7)$$

Proof. See Appendix B.2. □

4.1 Nonconvex setting

We now present our main convergence result for EFVFL.

Theorem 1. Let $\{\mathbf{x}^t\}$ be a sequence generated by Algorithm 1, \mathcal{C} be a contractive compressor (2), and $f^* > -\infty$. If (A1) to (A4) hold, then, for $0 < \eta \leq 1/(\sqrt{\rho_{\alpha 1}}L + L)$:

$$\frac{1}{T} \sum_{t=0}^{T-1} \mathbb{E}\|\nabla f(\mathbf{x}^t)\|^2 \leq \frac{2\Delta}{\eta T} + (1 + \eta L \rho_{\alpha 1}) \frac{\eta L \sigma^2}{B} + \rho_{\alpha 2} \frac{\mathbb{E}D^0}{T}, \quad (8)$$

where the expectation is over the randomness in \mathcal{C} and in $\{\mathcal{B}_t\}$, $\Delta := f(\boldsymbol{\theta}^0) - f^*$, and

$$\rho_{\alpha 1} := KH^4 \left(\frac{1 + \sqrt{1-\alpha}}{\alpha} - 1 \right)^2 \quad \text{and} \quad \rho_{\alpha 2} := \frac{KH^2L^2}{1 - \sqrt{1-\alpha}}.$$

Proof. See Appendix C.1. □

If the batch size is large enough, $B = \Omega(\sigma^2/\epsilon)$, the iteration complexity to reach $\frac{1}{T} \sum_{t=0}^{T-1} \mathbb{E}\|\nabla f(\boldsymbol{\theta}^t)\|^2 \leq \epsilon$ matches the $\mathcal{O}(1/T)$ rate of the centralized, uncompressed setting. Also, in the absence of compression ($\alpha = 1$ and $D^t = 0$), we recover that, for $\eta \in (0, 1/L]$, we can output an \mathbf{x}^{out} such that $\mathbb{E}\|\nabla f(\mathbf{x}^{\text{out}})\|^2 \leq \frac{2\Delta}{\eta T} + \frac{\eta L \sigma^2}{B}$. If we are also in the full-batch case ($\sigma = 0$), we recover the gradient descent bound exactly: $\mathbb{E}\|\nabla f(\mathbf{x}^{\text{out}})\|^2 \leq \frac{2\Delta}{\eta T}$.

Our results improve over the prior state-of-the-art compressed vertical FL (CVFL) (Castiglia et al., 2022), whose convergence results for a fixed stepsize is presented below:

$$\frac{1}{T} \sum_{t=0}^{T-1} \mathbb{E}\|\nabla f(\mathbf{x}^t)\|^2 \leq \frac{4\Delta}{\eta T} + \mathcal{O}\left(\frac{\eta L \sigma^2}{B}\right) + \mathcal{O}\left(\frac{1}{T} \sum_{t=0}^{T-1} D_d^t\right).$$

Note how, even for full-batch updates, the upper bound above does not go to zero as $T \rightarrow \infty$ unless $D_d^t \rightarrow 0$, where D_d^t is the distortion resulting from direct compression $D_d^t = \sum_{k=0}^K \|\mathcal{C}(\mathbf{H}_k(\mathbf{x}_k^t)) - \mathbf{H}_k(\mathbf{x}_k^t)\|^2$. That is, to achieve $\frac{1}{T} \sum_{t=0}^{T-1} \mathbb{E}\|\nabla f(\mathbf{x}^t)\|^2 \rightarrow 0$, CVFL requires a vanishing compression error, which necessitates that $\alpha \rightarrow 1$. This means that, despite reducing the total amount communications across the training, CVFL does not reduce the maximum amount of communications per round. In contrast, by allowing for nonvanishing compression, EFVFL ensures small communication cost at every round.

4.2 Under the PL inequality

In this section, we establish the linear convergence of EFVFL under the PL inequality (Polyak, 1963).

Assumption 5 (PL inequality). *We assume that there exists a positive constant μ such that*

$$\forall \mathbf{x} \in \mathbb{R}^d: \quad \|\nabla f(\mathbf{x})\|^2 \geq 2\mu(f(\mathbf{x}) - f^*). \quad (\text{A5})$$

We resort to the following Lyapunov function to show linear convergence:

$$V_t := \mathbb{E}f(\mathbf{x}^t) - f^* + c\mathbb{E}D^t, \quad (9)$$

where c is a positive constant. We now present Theorem 2.

Theorem 2. *Let $\{\mathbf{x}^t\}$ be a sequence generated by Algorithm 1, \mathcal{C} be a contractive compressor (2), and $f^* > -\infty$. If (A1) to (A5) hold, then, for η such that $\eta^2 L^2 (1 - \mu/L) + \eta\mu \leq \alpha^2$, we have:*

$$V_T \leq (1 - \eta\mu)^T V_0 + \mathcal{O}\left(\frac{\eta\sigma^2}{B}\right).$$

Proof. See Appendix C.2. □

Since $\mu \leq L$, we have that $\eta \in (0, 1/L)$ implies that $1 - \eta\mu \in (0, 1)$. Hence, EFVFL converges linearly to a $\mathcal{O}(\sigma^2)$ neighborhood around the global optimum.

5 Experiments

We compare EFVFL with two baselines: (1) standard VFL (SVFL), which corresponds to the method in Liu et al. (2022) and is mathematically equivalent to stochastic gradient descent when a single local update is used, and (2) CVFL (Castiglia et al., 2022), which recovers SVFL when an identity compressor is used (that is, without employing compression). All of our results correspond to the mean and standard deviation for five different seeds. We employ two popular compressors in our experiments.

- Top- k sparsification (Alistarh et al., 2018; Stich et al., 2018) is a map $\text{top}_k: \mathbb{R}^d \mapsto \mathbb{R}^d$ defined as

$$\text{top}_k(\mathbf{v}) := \mathbf{v} \odot \mathbf{u}(\mathbf{v}),$$

where \odot denotes the Hadamard product and $\mathbf{u}(\mathbf{v})$ is such that its entry i is 1 if v_i is one of the k largest entries of \mathbf{v} in absolute value and 0 otherwise. We have that (2) holds for $\alpha = k/d$.

- Stochastic quantization (Alistarh et al., 2017) is a map $\text{qsgd}_s: \mathbb{R}^d \mapsto \mathbb{R}^d$, with $s > 1$ quantization levels defined as

$$\text{qsgd}_s(\mathbf{v}) := \frac{\|\mathbf{v}\| \cdot \text{sign}(\mathbf{v})}{s\tau} \cdot \left\lfloor s \frac{|\mathbf{v}|}{\|\mathbf{v}\|} + \xi \right\rfloor,$$

where $\tau = 1 + \min\{d/s^2, \sqrt{d}/s\}$ and $\xi \sim \mathcal{U}([0, 1]^d)$, where \mathcal{U} denotes the uniform distribution. In practice, we are interested in values of s such that $s = 2^b$, where b is the number of bits. We have that (2) holds for $\alpha = 1/\tau$.

For the sake of the comparison with CVFL, we employ compressors $\mathcal{C} = \mathcal{C}_2 \circ \mathcal{C}_1$, where \mathcal{C}_2 is either $\text{top}_k(\mathbf{v})$ or qsgd_s and \mathcal{C}_1 selects the rows in \mathcal{B}^t , similarly to CVFL. Further, as explained in Section 3, our experiments focus on the compression of $\{\mathbf{H}_k(\mathbf{x}_k)\}_{k=1}^K$, and not \mathbf{x}_0 .

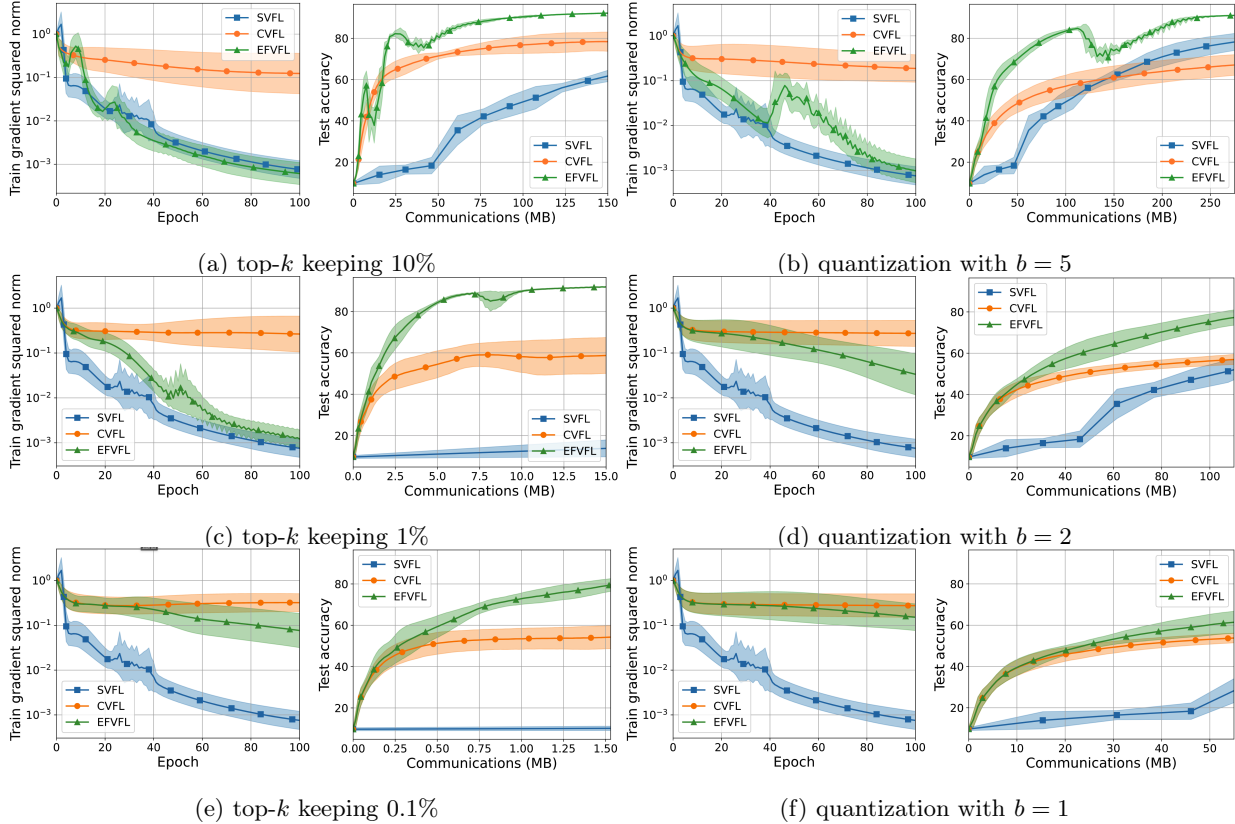


Figure 2: The (relative) training gradient squared norm with respect to epochs and test accuracy with respect to communication cost for the training of a shallow neural network on MNIST. On the left, CVFL and EFVFL employ top- k sparsification with a decreasing k across rows. On the right, they employ stochastic quantization with a decreasing number of bits across rows. SVFL is the same throughout.

5.1 Comparison with SVFL and CVFL

MNIST. We train a shallow neural network (one hidden layer) on the MNIST digit recognition dataset (LeCun et al., 1998). The 28×28 images in the original dataset \mathcal{D} are split into four local datasets \mathcal{D}_k of 14×14 images, its quadrants ($K = 4$). The local models $h_{k,n}$ are maps $\mathbf{v} \mapsto \text{sigmoid}(\mathbf{W}_{k1}\mathbf{v})$, with $\mathbf{W}_{k1} \in \mathbb{R}^{16 \times 196}$, and the server model is $(\mathbf{v}_1, \dots, \mathbf{v}_4) \mapsto \mathbf{W}_2(\sum_{k=1}^4 \mathbf{v}_k)$, with $\mathbf{W}_2 \in \mathbb{R}^{10 \times 16}$. We use cross-entropy loss. All three VFL optimizers use stepsize $\eta = 1$ and full-batch gradients. In Figure 2, we present the results for when EFVFL and CVFL employ top $_k$, keeping 10%, 1%, and 0.1% of the entries, and when they employ qsgd $_s$, sending $b \in \{5, 2, 1\}$ bits per entry, instead of the uncompressed $b = 32$. In both figures, we see that EFVFL outperforms SVFL and CVFL in communication efficiency. In terms of results per epoch, EFVFL significantly outperforms CVFL and, for a sufficiently large k (for top $_k$) or b (for qsgd $_s$) EFVFL achieves a similar performance to SVFL. As predicted in Section 4, the train gradient squared norm during training goes to zero for EFVFL, as it does for SVFL, but not for CVFL.

ModelNet10. We train a multi-view convolutional neural network (MVCNN) (Su et al., 2015) on ModelNet10 (Wu et al., 2015), a dataset of three-dimensional CAD models. We use a preprocessed version of ModelNet10, where each sample is represented by 12 two-dimensional views. We assign a view per client ($K = 12$). For all three VFL optimizers, we use a batch size $B = 128$, a stepsize $\eta = 0.004$, and a weight decay of 0.01. In Figure 3, we present the results for when EFVFL and CVFL employ top $_k$, keeping 20%, 2%, and 0.2% of the entries, and when they employ qsgd $_s$, with $b \in \{8, 4, 2\}$. We plot the train loss with respect to the number of epochs and the test accuracy with respect to the communication cost. We observe that, for EFVFL, the training loss decreases more rapidly than for CVFL. Further, if the compression is not

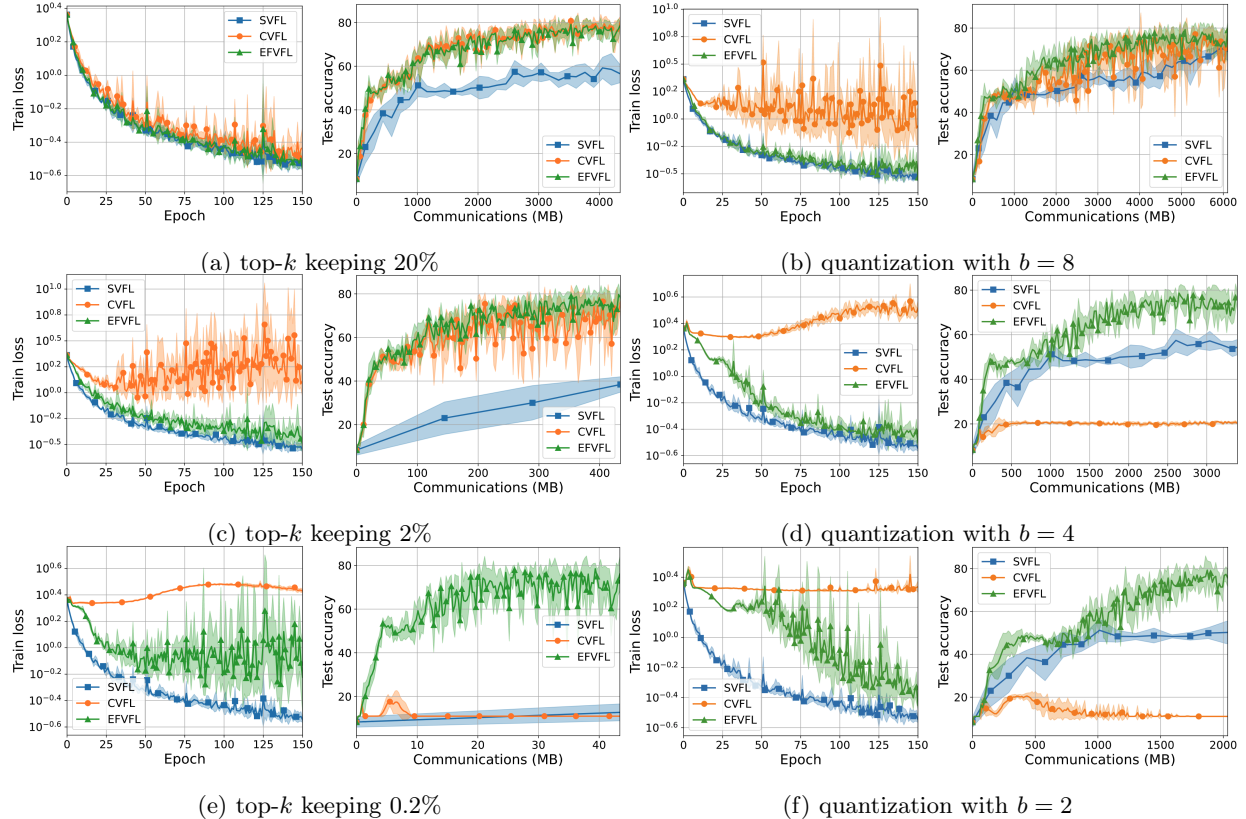


Figure 3: Train loss with respect to the number of epochs and test accuracy with respect to the communication cost for the training of an MVCNN on ModelNet10. On the left, CVFL and EFVFL employ top- k sparsification with a decreasing k across rows. On the right, they employ stochastic quantization with a decreasing number of bits across rows. SVFL is the same throughout.

excessively aggressive, EFVFL performs similarly to SVFL. In terms of communication efficiency, EFVFL outperforms both SVFL and CVFL.

CIFAR-10. We train a model based on a residual neural network, ResNet18 (He et al., 2016), on CIFAR-10 (Krizhevsky et al., 2009). More precisely, we divide each image into four quadrants and allocate one quadrant to each client ($K = 4$), with each client using a ResNet18 model as its local model. The server model is a multilayer perceptron with three layers. All three VFL optimizers use a batch size $B = 128$, a stepsize $\eta = 0.01$, and a weight decay of 0.01. In Figure 4, we present the results for when EFVFL and CVFL employ top- k , keeping 10%, 1%, and 0.1% of the entries, and when they employ qsgd_s, with $b \in \{4, 2, 1\}$. We plot the train loss with respect to the number of epochs and the test accuracy with respect to the communication cost. Regarding the results with respect to the number of epochs, EFVFL achieves a similar performance to that of SVFL, significantly outperforming CVFL. In terms of communication efficiency, EFVFL outperforms both SVFL and CVFL.

5.2 Performance under private labels

In this section, we run experiments on the adaption of EFVFL to handle private labels, proposed in Section 3.1.

In Castiglia et al. (2022), the authors assume that the labels are available at all clients and do not propose an adaptation of CVFL to deal with private labels. Yet, to get a baseline for a compressed VFL method allowing for label privacy, we adapt CVFL in a similar manner to how we adapt EFVFL (that is, sending back the derivative from the server to the clients, instead of ϕ_n and \mathbf{x}_0 , and without backpropagating through the compression operator).

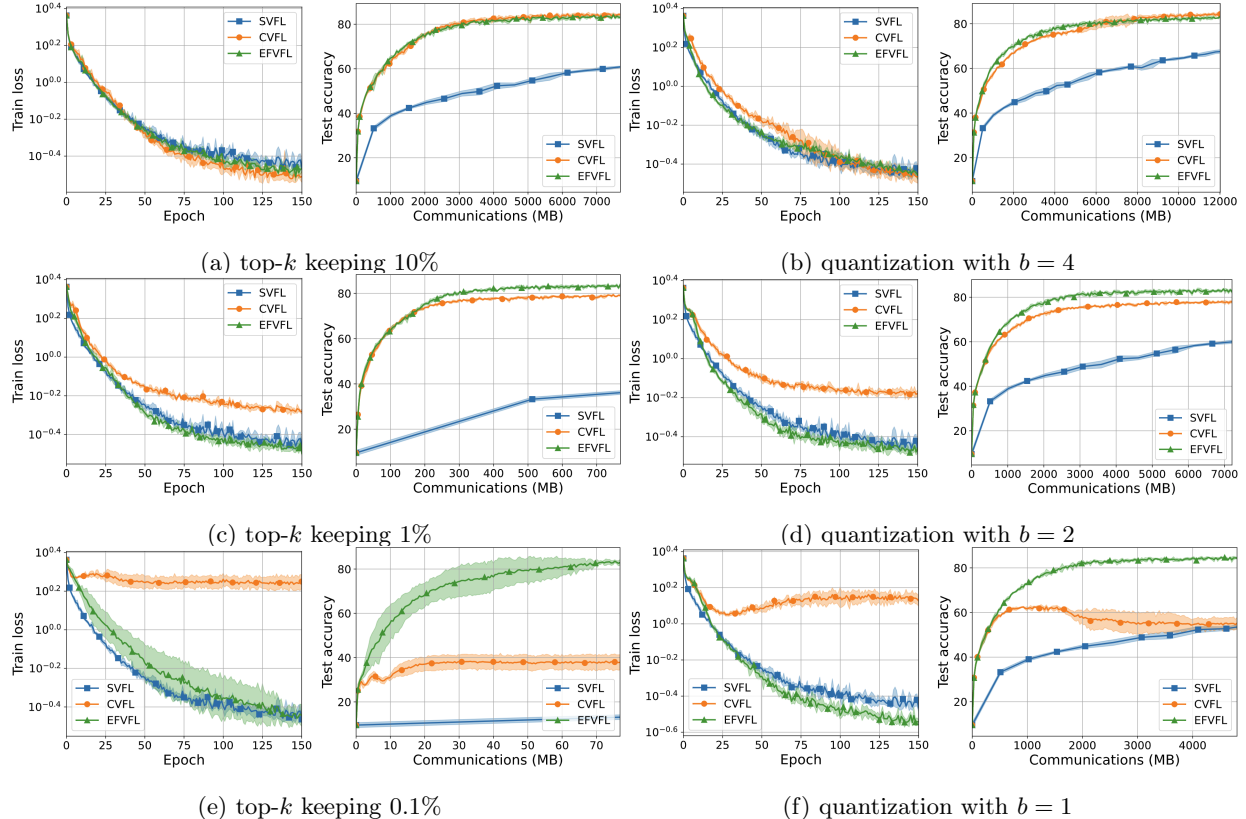


Figure 4: Train loss with respect to the number of epochs and the test accuracy with respect to the communication cost for the training of a ResNet18-based model on CIFAR-10. On the left, CVFL and EFVFL employ top- k sparsification with a decreasing k across rows. On the right, they employ stochastic quantization with a decreasing number of bits across rows. SVFL is the same throughout.

We run an experiment on MNIST, training the same shallow neural network as in model as in Section 5.1, with all the same settings, except for the use of batch size $B = 1024$. Further, we train another ResNet18-based model, now with a linear server model (a single layer), on CIFAR-100 (Krizhevsky et al., 2009). For all the optimizers, we use an initial stepsize of $\eta = 0.01$ and a cosine annealing scheduler with a minimum stepsize of $1/100$ the initial value and use a batch size $B = 128$ and a weight decay of 0.01. The compressed-communication methods employ top $_k$, keeping 5% of the entries.

In Figure 5, we observe that, although the modified EFVFL for handling private labels converges noticeably slower than the original method, it still performs effectively. For both the MNIST experiment and the CIFAR-100 experiment, we see that, while adapting CVFL to handle private labels leads to a severe drop in performance, EFVFL slows down much less noticeably. In fact, for the MNIST experiment, EFVFL with private labels still outperforms CVFL, even with public labels.

5.3 Performance under multiple local updates

As mentioned earlier, some VFL works employ $Q > 1$ local updates per round (Liu et al., 2022), using stale information from the other machines. We now show that, although our analysis focuses on the case where each client performs a single local update at each round of communications (that is, $Q = 1$), EFVFL performs well in the $Q > 1$ case too. In particular, to study the performance of EFVFL when carrying out multiple local updates, we train an MVCNN on ModelNet10 and a ResNet18 on CIFAR-10, on the same setups as in Section 5.1.

For ModelNet10, all three VFL optimizers use a batch size $B = 128$, a stepsize $\eta = 0.004$, and a weight decay of 0.01. Further, we use a learning rate scheduler, halving the learning rate at epochs 50 and 75.

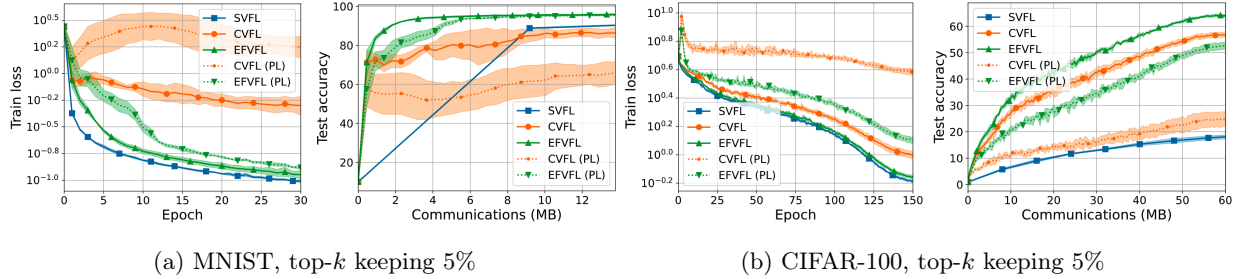


Figure 5: Train loss with respect to the number of epochs and test accuracy with respect to the communication cost for the training of a shallow neural network on MNIST and a ResNet18-based model on CIFAR-100. In the legend, PL stands for private labels. The communication compressed methods—CVFL, EFVFL, CVFL (PL), and EFVFL (PL)—employ top- k sparsification.

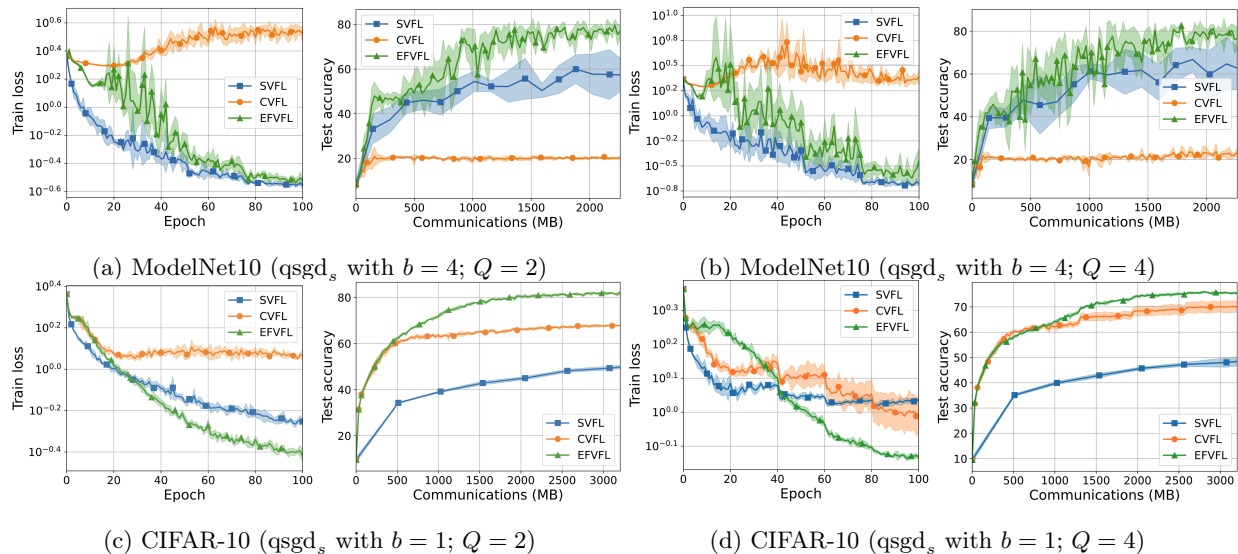


Figure 6: Train loss with respect to the number of epochs and test accuracy with respect to the communication cost for the training of a multi-view convolutional neural network on ModelNet10 and a residual neural network on CIFAR-10. CVFL and EFVFL use stochastic quantization. On the left, all three vertical FL optimizers use $Q = 2$ local updates and, on the right, they all use $Q = 4$ local updates.

The results are presented in Figure 6a and Figure 6b. For CIFAR-10, all three VFL optimizers use a batch size $B = 128$, a stepsize $\eta = 0.0025$, and a weight decay of 0.01. Further, we use a learning rate scheduler, halving the learning rate at epochs 40, 60, and 80. The results are presented in Figure 6c and Figure 6d.

For both ModelNet10 and CIFAR-10, we see that, similarly to the $Q = 1$ case, our method outperforms SVFL and CVFL in communication efficiency. In terms of results per epoch, EFVFL performs similarly to SVFL and significantly better than CVFL. Interestingly, for the CIFAR-10 task, EFVFL even outperforms SVFL with respect to the number of epochs. We suspect this may be due to the fact that compression helps to mitigate the overly greedy nature of the parallel updates based on stale information.

6 Conclusions

In this work, we proposed EFVFL, a method for compressed vertical federated learning. Our method leverages an error feedback mechanism to achieve a $\mathcal{O}(1/T)$ convergence rate, improving upon the state-of-the-art rate of $\mathcal{O}(1/\sqrt{T})$. Numerical experiments further demonstrate the faster convergence of our method. We further show that, under the PL inequality, our method converges linearly and introduce a modification of EFVFL supporting the use of private labels. In the future, it would be interesting to study the use of error feedback

based compression methods for VFL in the fully-decentralized and semi-decentralized settings, as well as combining it with privacy mechanisms, such as differential privacy.

Acknowledgements

This work is supported in part by the Fundação para a Ciência e a Tecnologia through the Carnegie Mellon Portugal Program; by the grants U.S. National Science Foundation CCF-2007911 and ECCS-2318441; and by the CMU-Portugal project CMU/TIC/0016/2021.

References

- D. Alistarh, D. Grubic, J. Li, R. Tomioka, and M. Vojnovic. QSGD: Communication-efficient SGD via gradient quantization and encoding. *Advances in neural information processing systems*, 30, 2017.
- D. Alistarh, T. Hoefer, M. Johansson, N. Konstantinov, S. Khirirat, and C. Renggli. The convergence of sparsified gradient methods. *Advances in Neural Information Processing Systems*, 31, 2018.
- A. Beznosikov, S. Horváth, P. Richtárik, and M. Safaryan. On biased compression for distributed learning. *Journal of Machine Learning Research*, 24(276):1–50, 2023.
- T. Castiglia, S. Wang, and S. Patterson. Flexible vertical federated learning with heterogeneous parties. *IEEE Transactions on Neural Networks and Learning Systems*, 2023.
- T. J. Castiglia, A. Das, S. Wang, and S. Patterson. Compressed-VFL: Communication-efficient learning with vertically partitioned data. In *International Conference on Machine Learning*, pages 2738–2766. PMLR, 2022.
- I. Ceballos, V. Sharma, E. Mugica, A. Singh, A. Roman, P. Vepakomma, and R. Raskar. SplitNN-driven vertical partitioning. *arXiv:2008.04137*, 2020.
- T. Chen, X. Jin, Y. Sun, and W. Yin. VAFI: a method of vertical asynchronous federated learning. *arXiv:2007.06081*, 2020.
- Y. Cheng, Y. Liu, T. Chen, and Q. Yang. Federated learning for privacy-preserving AI. *Communications of the ACM*, 63(12):33–36, 2020.
- J. Dean, G. Corrado, R. Monga, K. Chen, M. Devin, M. Mao, M. Ranzato, A. Senior, P. Tucker, K. Yang, et al. Large scale distributed deep networks. *Advances in neural information processing systems*, 25, 2012.
- F. Haddadpour, M. M. Kamani, A. Mokhtari, and M. Mahdavi. Federated learning with compression: Unified analysis and sharp guarantees. In *International Conference on Artificial Intelligence and Statistics*, pages 2350–2358. PMLR, 2021.
- K. He, X. Zhang, S. Ren, and J. Sun. Deep residual learning for image recognition. In *Proceedings of the IEEE conference on computer vision and pattern recognition*, 2016.
- Y. Hu, D. Niu, J. Yang, and S. Zhou. Fdml: A collaborative machine learning framework for distributed features. In *Proceedings of the 25th ACM SIGKDD International Conference on Knowledge Discovery & Data Mining*, pages 2232–2240, 2019.
- A. Khan, M. ten Thij, and A. Wilbik. Communication-efficient vertical federated learning. *Algorithms*, 15(8): 273, 2022.
- A. Koloskova, S. Stich, and M. Jaggi. Decentralized stochastic optimization and gossip algorithms with compressed communication. In *International Conference on Machine Learning*, pages 3478–3487. PMLR, 2019.
- A. Krizhevsky, G. Hinton, et al. Learning multiple layers of features from tiny images. 2009.

- Y. LeCun, L. Bottou, Y. Bengio, and P. Haffner. Gradient-based learning applied to document recognition. *Proceedings of the IEEE*, 86(11):2278–2324, 1998.
- M. Li, Y. Chen, Y. Wang, and Y. Pan. Efficient asynchronous vertical federated learning via gradient prediction and double-end sparse compression. In *2020 16th international conference on control, automation, robotics and vision (ICARCV)*, pages 291–296. IEEE, 2020.
- X. Lian, C. Zhang, H. Zhang, C.-J. Hsieh, W. Zhang, and J. Liu. Can decentralized algorithms outperform centralized algorithms? A case study for decentralized parallel stochastic gradient descent. *Advances in Neural Information Processing Systems*, 30, 2017.
- Y. Liu, X. Zhang, Y. Kang, L. Li, T. Chen, M. Hong, and Q. Yang. FedBCD: A communication-efficient collaborative learning framework for distributed features. *IEEE Transactions on Signal Processing*, 70: 4277–4290, 2022.
- Y. Liu, Y. Kang, T. Zou, Y. Pu, Y. He, X. Ye, Y. Ouyang, Y.-Q. Zhang, and Q. Yang. Vertical federated learning: Concepts, advances, and challenges. *IEEE Transactions on Knowledge and Data Engineering*, 2024.
- B. McMahan, E. Moore, D. Ramage, S. Hampson, and B. A. y Arcas. Communication-efficient learning of deep networks from decentralized data. In *Artificial intelligence and statistics*, pages 1273–1282. PMLR, 2017.
- B. T. Polyak. Gradient methods for the minimisation of functionals. *USSR Computational Mathematics and Mathematical Physics*, 3(4):864–878, 1963.
- P. Richtárik, I. Sokolov, and I. Fatkhullin. EF21: A new, simpler, theoretically better, and practically faster error feedback. *Advances in Neural Information Processing Systems*, 34:4384–4396, 2021.
- A. Sapio, M. Canini, C.-Y. Ho, J. Nelson, P. Kalnis, C. Kim, A. Krishnamurthy, M. Moshref, D. Ports, and P. Richtárik. Scaling distributed machine learning with in-network aggregation. In *18th USENIX Symposium on Networked Systems Design and Implementation (NSDI 21)*, pages 785–808, 2021.
- F. Seide, H. Fu, J. Droppo, G. Li, and D. Yu. 1-bit stochastic gradient descent and its application to data-parallel distributed training of speech dnns. In *Fifteenth annual conference of the international speech communication association*, 2014.
- S. U. Stich, J.-B. Cordonnier, and M. Jaggi. Sparsified SGD with memory. *Advances in Neural Information Processing Systems*, 31, 2018.
- H. Su, S. Maji, E. Kalogerakis, and E. Learned-Miller. Multi-view convolutional neural networks for 3D shape recognition. In *Proceedings of the IEEE international conference on computer vision*, 2015.
- P. Valdeira, Y. Chi, C. Soares, and J. Xavier. A multi-token coordinate descent method for semi-decentralized vertical federated learning. *arXiv:2309.09977*, 2023.
- P. Valdeira, J. Xavier, C. Soares, and Y. Chi. Communication-efficient vertical federated learning via compressed error feedback. *32nd European Signal Processing Conference (EUSIPCO)*, 2024.
- Z. Wu, S. Song, A. Khosla, F. Yu, L. Zhang, X. Tang, and J. Xiao. 3D ShapeNets: A deep representation for volumetric shapes. In *Proceedings of the IEEE conference on computer vision and pattern recognition*, 2015.
- C. Xie, S. Koyejo, and I. Gupta. Asynchronous federated optimization. *arXiv:1903.03934*, 2019.
- L. Yang, D. Chai, J. Zhang, Y. Jin, L. Wang, H. Liu, H. Tian, Q. Xu, and K. Chen. A survey on vertical federated learning: From a layered perspective. *arXiv:2304.01829*, 2023.
- B. Ying, K. Yuan, and A. H. Sayed. Supervised learning under distributed features. *IEEE Transactions on Signal Processing*, 67(4):977–992, 2018.

A Preliminaries

If a function is L -smooth (A1), then the following quadratic upper bound holds:

$$\forall \mathbf{x}, \mathbf{y} \in \mathbb{R}^d: \quad f(\mathbf{y}) \leq f(\mathbf{x}) + \nabla f(\mathbf{x})^\top (\mathbf{y} - \mathbf{x}) + \frac{L}{2} \|\mathbf{x} - \mathbf{y}\|^2. \quad (10)$$

It follows from Assumption (2) that the following inequality holds:

$$\|\mathbf{H}_k(\mathbf{x}) - \mathbf{H}_k(\mathbf{y})\| \leq H \|\mathbf{x} - \mathbf{y}\|, \quad \forall \mathbf{x}, \mathbf{y} \in \mathbb{R}^{d_k}. \quad (11)$$

Letting $\epsilon > 0$, we use the following standard inequality in our analysis:

$$\forall \mathbf{x}, \mathbf{y} \in \mathbb{R}^d: \quad \|\mathbf{x} + \mathbf{y}\|^2 \leq (1 + \epsilon) \|\mathbf{x}\|^2 + (1 + \epsilon^{-1}) \|\mathbf{y}\|^2. \quad (12)$$

We define the distortion associated with block k at time t as

$$D_k^t := \|\mathbf{G}_k^t - \mathbf{H}_k(\mathbf{x}_k^t)\|^2$$

and, recall, we denote the total distortion at time t as $D^t = \sum_{k=0}^K D_k^t$.

In Section 4, we introduced the following sigma-algebra

$$\mathcal{F}_t = \sigma(\mathbf{G}^0, \mathbf{x}^1, \mathbf{G}^1, \dots, \mathbf{x}^t, \mathbf{G}^t),$$

where $\mathbf{G}^t = \{\mathbf{G}_0^t, \dots, \mathbf{G}_K^t\}$. We now further define

$$\mathcal{F}'_t := \sigma(\mathbf{G}^0, \mathbf{x}^1, \mathbf{G}^1, \dots, \mathbf{x}^t, \mathbf{G}^t, \mathbf{x}^{t+1}).$$

Recall that we let \mathbb{E}_{σ_t} denote the conditional expectation $\mathbb{E}[\cdot \mid \sigma_t]$ and that $\delta := (1 - \alpha) \in [0, 1)$.

Note that, while we write our proofs for Algorithm 1, they can be easily adjusted to cover Algorithm 2. To do so, it suffices to adjust the notation, replacing \mathbf{g}^t and $\tilde{\mathbf{g}}^t$ by ∇_k^t and $\tilde{\nabla}_k^t$, respectively, and to make minor changes to the proof of Lemma 1, which cause the constant K in Lemma 1 to be replaced with $K + 1$. This, in turn, leads to a similar adjustment in the constants of our main theorems.

B Supporting Lemmas

B.1 Proof of Lemma 1

Decoupling the offset across blocks, we get that

$$\begin{aligned} & \|\mathbf{g}^t - \nabla f(\mathbf{x}^t)\|^2 \\ &= \sum_{k=0}^K \|\mathbf{g}_k^t - \nabla_k f(\mathbf{x}_k)\|^2, \\ &\leq \sum_{k=0}^K \|\nabla \mathbf{H}_k(\mathbf{x}_k)\|^2 \left\| \tilde{\nabla}_k^t \Phi - \nabla_k \Phi(\{\mathbf{H}_k(\mathbf{x}_k^t)\}_{k=0}^K) \right\|^2, \end{aligned}$$

where we use the chain rule and the fact that $\|\mathbf{A}\mathbf{x}\| \leq \|\mathbf{A}\| \|\mathbf{x}\|$. Now, it follows from the bounded gradient assumption (A2) on $\{\mathbf{H}_k\}$ and the L -smoothness (A1) of Φ that

$$\|\mathbf{g}^t - \nabla f(\mathbf{x}^t)\|^2 \leq H^2 L^2 \sum_{k=0}^K \sum_{j \neq k} \|\mathbf{G}_j^t - \mathbf{H}_j(\mathbf{x}_j^t)\|^2$$

$$\begin{aligned}
&= H^2 L^2 \sum_{k=0}^K \sum_{j \neq k} D_j^t \\
&= KH^2 L^2 D^t,
\end{aligned}$$

as we set out to prove. For Algorithm 2, the sum $\sum_{j \neq k}$ would instead be $\sum_{j=1}^K$, leading to $\|\mathbf{g}^t - \nabla f(\mathbf{x}^t)\|^2 \leq (K+1)H^2 L^2 D^t$. However, note that, for Algorithm 2, $D_0^t = 0$.

B.2 Proof of Lemma 2

It follows from the definition of distortion and from the update of our compression estimate that

$$\begin{aligned}
\mathbb{E}_{\mathcal{F}_t'} [D_k^{t+1}] &= \mathbb{E}_{\mathcal{F}_t'} \|\mathbf{G}_k^{t+1} - \mathbf{H}_k(\mathbf{x}_k^{t+1})\|^2 \\
&= \mathbb{E}_{\mathcal{F}_t'} \|\mathbf{G}_k^t + \mathcal{C}(\mathbf{H}_k(\mathbf{x}_k^{t+1}) - \mathbf{G}_k^t) - \mathbf{H}_k(\mathbf{x}_k^{t+1})\|^2.
\end{aligned}$$

Now, from the definition of contractive compressor (2) and from (12), we have that

$$\begin{aligned}
\mathbb{E}_{\mathcal{F}_t'} [D_k^{t+1}] &\leq \delta \|\mathbf{G}_k^t - \mathbf{H}_k(\mathbf{x}_k^{t+1})\|^2 \\
&\leq \delta(1+\epsilon) \|\mathbf{G}_k^t - \mathbf{H}_k(\mathbf{x}_k^t)\|^2 \\
&\quad + \delta(1+\epsilon^{-1}) \|\mathbf{H}_k(\mathbf{x}_k^{t+1}) - \mathbf{H}_k(\mathbf{x}_k^t)\|^2.
\end{aligned}$$

Further, from the bounded gradient assumption—in particular, from (11)—we arrive at

$$\begin{aligned}
\mathbb{E}_{\mathcal{F}_t'} [D_k^{t+1}] &\leq \delta(1+\epsilon)D_k^t + \delta(1+\epsilon^{-1})H^2 \|\mathbf{x}_k^{t+1} - \mathbf{x}_k^t\|^2 \\
&= \delta(1+\epsilon)D_k^t + \delta(1+\epsilon^{-1})\eta^2 H^2 \|\tilde{\mathbf{g}}_k^t\|^2,
\end{aligned}$$

where, recall, $\tilde{\mathbf{g}}_k^t$ is our (possibly stochastic) update vector. Summing over $k = 0, 1, \dots, K$ and taking the nonconditional expectation of both sides of the inequality, we get that

$$\mathbb{E}D^{t+1} \leq \delta(1+\epsilon)\mathbb{E}D^t + \delta(1+\epsilon^{-1})\eta^2 H^2 \mathbb{E}\|\tilde{\mathbf{g}}^t\|^2.$$

Lastly, using the fact that, under (A3), (A4) is equivalent to $\mathbb{E}\|\tilde{\mathbf{g}}^t\|^2 \leq \mathbb{E}\|\mathbf{g}^t\|^2 + \frac{\sigma^2}{B}$, we arrive at (7).

C Main Theorems

First, let us define some shorthand notation for terms we will be using throughout our proof, whose expectation is with respect to the (possible) randomness in the compression across all steps:

$$\begin{aligned}
(\text{compression error}) \quad \Omega_1^t &:= \mathbb{E}D^t, \\
(\text{surrogate norm}) \quad \Omega_2^t &:= \mathbb{E}\|\mathbf{g}^t\|^2.
\end{aligned}$$

C.1 Proof of Theorem 1

From the L -smoothness of f —more specifically, from (10)—we have that

$$f(\mathbf{x}^{t+1}) - f(\mathbf{x}^t) \leq \langle \nabla f(\mathbf{x}^t), \mathbf{x}^{t+1} - \mathbf{x}^t \rangle + \frac{L}{2} \|\mathbf{x}^{t+1} - \mathbf{x}^t\|^2 = -\eta \langle \nabla f(\mathbf{x}^t), \tilde{\mathbf{g}}^t \rangle + \frac{\eta^2 L}{2} \|\tilde{\mathbf{g}}^t\|^2.$$

Taking the conditional expectation over the batch selection, it follows from the unbiasedness of $\tilde{\mathbf{g}}^t$ (A3) that

$$\mathbb{E}_{\mathcal{F}_t} f(\mathbf{x}^{t+1}) - f(\mathbf{x}^t) \leq -\eta \langle \nabla f(\mathbf{x}^t), \mathbf{g}^t \rangle + \frac{\eta^2 L}{2} \mathbb{E}_{\mathcal{F}_t} \|\tilde{\mathbf{g}}^t\|^2.$$

From (A4), we have that $\mathbb{E}_{\mathcal{F}_t} \|\tilde{\mathbf{g}}^t - \mathbf{g}^t\|^2 \leq \frac{\sigma^2}{B}$, which, under (A3), is equivalent to $\mathbb{E}_{\mathcal{F}_t} \|\tilde{\mathbf{g}}^t\|^2 \leq \|\mathbf{g}^t\|^2 + \frac{\sigma^2}{B}$, so

$$\begin{aligned} \mathbb{E}_{\mathcal{F}_t} f(\mathbf{x}^{t+1}) - f(\mathbf{x}^t) &\leq -\eta \langle \nabla f(\mathbf{x}^t), \mathbf{g}^t \rangle + \frac{\eta^2 L}{2} \|\mathbf{g}^t\|^2 + \frac{\eta^2 L \sigma^2}{2B} \\ &= -\frac{\eta}{2} \|\nabla f(\mathbf{x}^t)\|^2 - \frac{\eta}{2} (1 - \eta L) \|\mathbf{g}^t\|^2 + \frac{\eta}{2} \|\mathbf{g}^t - \nabla f(\mathbf{x}^t)\|^2 + \frac{\eta^2 L \sigma^2}{2B}, \end{aligned}$$

where the last equation follows from the polarization identity $\langle a, b \rangle = \frac{1}{2}(\|a\|^2 + \|b\|^2 - \|a - b\|^2)$. Now, using our surrogate offset bound (6) and taking the (non-conditional) expectation, we get that:

$$\mathbb{E} f(\mathbf{x}^{t+1}) - \mathbb{E} f(\mathbf{x}^t) \leq -\frac{\eta}{2} \mathbb{E} \|\nabla f(\mathbf{x}^t)\|^2 - \frac{\eta}{2} (1 - \eta L) \mathbb{E} \|\mathbf{g}^t\|^2 + \frac{\eta K H^2 L^2}{2} \mathbb{E} D^t + \frac{\eta^2 L \sigma^2}{2B}. \quad (13)$$

Using the Ω_1^t and Ω_2^t notation defined earlier, we rewrite (7) and (13), respectively, as

$$\begin{cases} \Omega_1^{t+1} \leq \delta(1 + \epsilon) \Omega_1^t + \delta(1 + \epsilon^{-1}) \eta^2 H^2 \Omega_2^t + \frac{\delta(1 + \epsilon^{-1}) \eta^2 H^2 \sigma^2}{B}, \\ \mathbb{E} f(\mathbf{x}^{t+1}) - \mathbb{E} f(\mathbf{x}^t) \leq -\frac{\eta}{2} \mathbb{E} \|\nabla f(\mathbf{x}^t)\|^2 + \frac{\eta K H^2 L^2}{2} \Omega_1^t - \frac{\eta}{2} (1 - \eta L) \Omega_2^t + \frac{\eta^2 L \sigma^2}{2B}. \end{cases}$$

Multiplying the first inequality by a positive constant w and adding it to the second one, we get

$$\mathbb{E} f(\mathbf{x}^{t+1}) - \mathbb{E} f(\mathbf{x}^t) + w \Omega_1^{t+1} - \psi_1(w) \Omega_1^t \leq -\frac{\eta}{2} \mathbb{E} \|\nabla f(\mathbf{x}^t)\|^2 + \psi_2(w) \Omega_2^t + \left(w \delta (1 + \epsilon^{-1}) H^2 + \frac{L}{2} \right) \frac{\eta^2 \sigma^2}{B}, \quad (14)$$

where

$$\psi_1(w) := w \delta (1 + \epsilon) + \frac{\eta K H^2 L^2}{2} \quad \text{and} \quad \psi_2(w) := w \delta (1 + \epsilon^{-1}) \eta^2 H^2 - \frac{\eta}{2} (1 - \eta L).$$

Looking at (14), we see that, if $\psi_2(w) \leq 0$, we can drop the Ω_2^t term. Further, if $\psi_1(w) \leq w$, we can telescope the Ω_1^t term as we sum the inequalities for $t = 0, \dots, T - 1$, as we do for the $\mathbb{E} f(\mathbf{x}^t)$ terms. We thus get that:

$$\frac{1}{T} \sum_{t=0}^{T-1} \mathbb{E} \|\nabla f(\mathbf{x}^t)\|^2 \leq \frac{2(f(\mathbf{x}^0) - \mathbb{E} f(\mathbf{x}^T))}{\eta T} + \frac{2w(\Omega_1^0 - \Omega_1^T)}{\eta T} + (2w\delta(1 + \epsilon^{-1})H^2 + L) \frac{\eta^2 \sigma^2}{B}, \quad (15)$$

for

$$w \in \mathcal{W}_\epsilon := \left\{ w : \frac{\eta K H^2 L^2}{2(1 - \delta(1 + \epsilon))} \leq w \leq \frac{1 - \eta L}{2\eta H^2 \delta(1 + \epsilon^{-1})} \right\},$$

where the lower bound follows from $\psi_1(w) \leq w$ and the upper bound from $\psi_2(w) \leq 0$.

Bounding η and choosing ϵ . To ensure that \mathcal{W}_ϵ is not empty, we need

$$\eta^2 \gamma(\epsilon) L^2 + \eta L \leq 1 \quad \text{where} \quad \gamma(\epsilon) := K H^4 \frac{\delta(1 + \epsilon^{-1})}{1 - \delta(1 + \epsilon)}.$$

From Lemma 5 of Richtárik et al. (2021), we know that, if $a, b > 0$, then $0 \leq \eta \leq \frac{1}{\sqrt{a+b}}$ implies $a\eta^2 + b\eta \leq 1$. Thus, we can ensure that \mathcal{W}_ϵ is not empty by requiring

$$\eta \leq \frac{1}{\sqrt{\gamma(\epsilon)L^2 + L}} = \left(\sqrt{\gamma(\epsilon)L} + L \right)^{-1}.$$

Further, to ensure that all $w \in \mathcal{W}_\epsilon$ are positive, we need $\delta(1 + \epsilon) < 1$, which holds for $\epsilon < \frac{1-\delta}{\delta}$. Thus, to have the largest upper bound possible on the stepsize η , we want ϵ to be the solution to the following optimization problem, solved in Lemma 3 of Richtárik et al. (2021):

$$\epsilon^* := \operatorname{argmin}_\epsilon \left\{ \tilde{\gamma}(\epsilon) := \frac{\delta(1 + \epsilon^{-1})}{1 - \delta(1 + \epsilon)} : 0 < \epsilon < \frac{1 - \delta}{\delta} \right\} = \frac{1}{\sqrt{\delta}} - 1.$$

It follows that $\sqrt{\tilde{\gamma}(\epsilon^*)} = \frac{1 + \sqrt{1 - \alpha}}{\alpha} - 1$ and thus $\gamma(\epsilon^*) = K H^4 \left(\frac{1 + \sqrt{1 - \alpha}}{\alpha} - 1 \right)^2 =: \rho_{\alpha 1}$. We therefore need

$$\eta \leq \left(\sqrt{\gamma(\epsilon^*)L} + L \right)^{-1} = \left(\sqrt{\rho_{\alpha 1}L} + L \right)^{-1}.$$

Note that, for $\alpha = 1$, we recover $\eta \leq 1/L$.

Choosing w . Now, since $f^* \leq f(\mathbf{x})$ for all \mathbf{x} and $\Omega_1^T \geq 0$, we have from (15) that

$$\forall w \in \mathcal{W}_\epsilon: \quad \frac{1}{T} \sum_{t=0}^{T-1} \mathbb{E} \|\nabla f(\mathbf{x}^t)\|^2 \leq \frac{2\Delta}{\eta T} + \frac{2w\Omega_1^0}{\eta T} + (2w\delta(1+\epsilon^{-1})H^2 + L) \frac{\eta\sigma^2}{B},$$

where $\Delta := f(\mathbf{x}^0) - f^*$. From the inequality above, we see that we want $w \in \mathcal{W}_\epsilon$ to be as small as possible. Therefore, we take w to be the lower bound in \mathcal{W}_ϵ . Since $1 - \delta(1 + \epsilon^*) = 1 - \sqrt{\delta}$, this corresponds to setting $w = \frac{\eta KH^2 L^2}{2(1-\sqrt{\delta})}$. Recalling that $\Omega_1^t = \mathbb{E}D^t$ and $\delta = 1 - \alpha$, we thus arrive at (8):

$$\frac{1}{T} \sum_{t=0}^{T-1} \mathbb{E} \|\nabla f(\mathbf{x}^t)\|^2 \leq \frac{2\Delta}{\eta T} + \frac{KH^2 L^2}{1 - \sqrt{1 - \alpha}} \cdot \frac{\mathbb{E}D^0}{T} + (\eta L \rho_{\alpha 1} + 1) \frac{\eta L \sigma^2}{B}.$$

C.2 Proof of Theorem 2

Recall that, using the Ω_1^t and Ω_2^t notation, we can rewrite (7) and (13), respectively, as

$$\begin{cases} \Omega_1^{t+1} \leq \delta(1+\epsilon)\Omega_1^t + \delta(1+\epsilon^{-1})\eta^2 H^2 \Omega_2^t + \frac{\delta(1+\epsilon^{-1})\eta^2 H^2 \sigma^2}{B}, \\ \mathbb{E}f(\mathbf{x}^{t+1}) - \mathbb{E}f(\mathbf{x}^t) \leq -\frac{\eta}{2} \mathbb{E} \|\nabla f(\mathbf{x}^t)\|^2 + \frac{\eta KH^2 L^2}{2} \Omega_1^t - \frac{\eta}{2}(1-\eta L)\Omega_2^t + \frac{\eta^2 L \sigma^2}{2B}. \end{cases}$$

Now, from our earlier introduced Lyapunov function (9), $V_t = \mathbb{E}f(\mathbf{x}^t) - f^* + c\Omega_1^t$, we have that:

$$\begin{aligned} V_{t+1} &= \mathbb{E}f(\mathbf{x}^{t+1}) - f^* + c\Omega_1^{t+1} \\ &\stackrel{(i)}{\leq} \mathbb{E}f(\mathbf{x}^t) - f^* - \frac{\eta}{2} \mathbb{E} \|\nabla f(\mathbf{x}^t)\|^2 + \left(\frac{\eta KH^2 L^2}{2} + c\delta(1+\epsilon) \right) \Omega_1^t + \psi_2(c)\Omega_2^t + (L + 2c\delta(1+\epsilon^{-1})H^2) \frac{\eta^2 \sigma^2}{2B} \\ &\stackrel{(ii)}{\leq} (1-\eta\mu)(\mathbb{E}f(\mathbf{x}^t) - f^*) + \left(\frac{\eta KH^2 L^2}{2} + c\delta(1+\epsilon) \right) \Omega_1^t + \psi_2(c)\Omega_2^t + (L + 2c\delta(1+\epsilon^{-1})H^2) \frac{\eta^2 \sigma^2}{2B} \\ &= (1-\eta\mu)V_t + \underbrace{\left(\frac{\eta KH^2 L^2}{2} + c\delta(1+\epsilon) - c(1-\eta\mu) \right)}_{=:\psi_3(c)} \Omega_1^t + \psi_2(c)\Omega_2^t + (L + 2c\delta(1+\epsilon^{-1})H^2) \frac{\eta^2 \sigma^2}{2B}, \end{aligned}$$

where (i) follows from (7), (13), $c > 0$, and $\psi_2(w) = w\delta(1+\epsilon^{-1})\eta^2 H^2 - \frac{\eta}{2}(1-\eta L)$ and (ii) follows from the PL inequality (A5). Looking the inequality above, we see that, if there is a c such that $\psi_2(c), \psi_3(c) \leq 0$, then

$$V_{t+1} \leq (1-\eta\mu)V_t + (L + 2cH^2\delta(1+\epsilon^{-1})) \frac{\eta^2 \sigma^2}{2B}. \quad (16)$$

Note that, similarly to what we had in the proof for Theorem 1, $\psi_2(c) \leq 0$ corresponds to an upper bound on c , while $\psi_3(c) \leq 0$ corresponds to a lower bound on c . We therefore want $c \in \mathcal{W}'_\epsilon$, where

$$\mathcal{W}'_\epsilon := \left\{ c: \frac{\eta KH^2 L^2}{2(1-\delta(1+\epsilon)-\eta\mu)} \leq c \leq \frac{1-\eta L}{2\eta\delta(1+\epsilon^{-1})H^2} \right\}.$$

Recurring (16), we get

$$\begin{aligned} V_T &\leq (1-\eta\mu)^T V_0 + (L + 2cH^2\delta(1+\epsilon^{-1})) \frac{\eta^2 \sigma^2}{2B} \sum_{t=0}^{T-1} (1-\eta\mu)^t \\ &\leq (1-\eta\mu)^T V_0 + (L + 2cH^2\delta(1+\epsilon^{-1})) \frac{\eta\sigma^2}{2B\mu}, \end{aligned}$$

where the second inequality follows from the sum of a geometric series, arriving at the result we set out to prove.

Choosing ϵ and bounding η so that \mathcal{W}'_ϵ is nonempty. Note that the lower bound defining \mathcal{W}'_ϵ is positive if $\eta < \frac{1-\delta(1+\epsilon)}{\mu}$, where $1 - \delta(1 + \epsilon) > 0$ as long as $\epsilon < \frac{1-\delta}{\delta}$. Further, \mathcal{W}'_ϵ is not empty, as long as

$$\frac{\eta KH^2 L^2}{2(1 - \delta(1 + \epsilon) - \eta\mu)} \leq \frac{1 - \eta L}{2\eta\delta(1 + \epsilon^{-1})H^2},$$

which is equivalent to

$$\eta^2 L^2 (\beta_\epsilon(\alpha) KH^4 - \mu/L) + \eta L(\theta_\epsilon(\alpha) + \mu/L) \leq \theta_\epsilon(\alpha),$$

where

$$\theta_\epsilon(\alpha) = 1 - (1 - \alpha)(1 + \epsilon) \quad \text{and} \quad \beta_\epsilon(\alpha) = (1 - \alpha)(1 + \epsilon^{-1}).$$

If $\epsilon \leq \min\left\{\frac{1-\alpha}{\alpha}, \frac{\alpha}{1-\alpha}\right\}$, we have that $\beta_\epsilon(\alpha) \geq 1$ and $\theta_\epsilon(\alpha) \geq 0$ for all α . It follows from $\beta_\epsilon(\alpha) \geq 1$ that $\beta_\epsilon(\alpha) \geq 1KH^4 \geq KH^4 \geq H^4 \geq 1$, where the last inequality follows from (A2) holding for \mathbf{H}_0 . We thus get that

$$\eta^2 L^2 (1 - \mu/L) + \eta L(\mu/L) \leq \theta_\epsilon(\alpha). \quad (17)$$

Choosing ϵ to be

$$\epsilon^* = \begin{cases} \alpha, & 0 < \alpha \leq 1/2, \\ 1 - \alpha, & 1/2 < \alpha \leq 1, \end{cases}$$

we get that

$$\theta_{\epsilon^*}(\alpha) = \begin{cases} \alpha^2, & 0 < \alpha \leq 1/2, \\ -1 + 3\alpha - \alpha^2, & 1/2 < \alpha \leq 1. \end{cases}$$

Since $\alpha^2 \leq -1 + 3\alpha - \alpha^2$ for $\alpha \in (1/2, 1]$, we have that $\alpha^2 \leq \theta_{\epsilon^*}(\alpha)$ for all $\alpha \in (0, 1]$. Thus, (17) holds if

$$\eta^2 L^2 (1 - \mu/L) + \eta L(\mu/L) \leq \alpha^2. \quad (18)$$

Further, from (A1) and (A5), we get that $0 \leq \mu/L \leq 1$. Therefore, for a sufficiently small η , there exists a positive $c \in \mathcal{W}'_\epsilon$ such that $\psi_2(c), \psi_3(c) \leq 0$. Lastly, note that we can also guarantee that $\eta < \frac{1-\delta(1+\epsilon^*)}{\mu} = \theta_{\epsilon^*}(\alpha)/\mu$ by having $\eta < \alpha^2/\mu$, which follows from (18). We thus conclude our proof.